Supporting Information

Bacterial-Derived, Compressible, and Hierarchical Porous Carbon for High-Performance Potassium-Ion Batteries

Hongyan Li[1#], Zheng Cheng[1#], Qing Zhang[1], Avi Natan[1], Yang Yang[1], Daxian Cao[1], Hongli Zhu[*,1]

[1]Department of Mechanical and Industrial Engineering, Northeastern University, Boston, Massachusetts 02115, United States.

*Dr. Hongli Zhu E-mail: h.zhu@neu.edu

[#] These authors contributed equally.

Contents list

I. Experimental Procedure:

1. Chemicals

The BC pellicles with fiber content of ~0.5 wt% were generated by a acetobacter xylinum fermentation process. All other chemicals were analytical grade and used as received without further purification. All aqueous solutions were prepared with ultrapure water (>18.2 MΩ cm) from a Milli-Q Plus system (Millipore). All glassware used in the following procedures were cleaned in a bath of freshly prepared HCl:HNO_3 (3:1) and rinsed thoroughly with ultrapure water prior to use.

2. Preparation of carbon nanofiber foam (CNFF)

The BC pellicles were purified by soaking in 0.2 mol L^{-1} NaOH 60 ^{o}C for 2h and then rinsed several times in deionized water for five days. Then, the pellicles were cut into rectangular shape (50 mm×40 mm×18 mm), frozen by liquid nitrogen, and then freeze-dried for 72 h to obtain the BC aerogel.[1] The obtained BC aerogels were transferred into a tube furnace for carbonization under nitrogen atmosphere. The BC precursors were heated to 240 ^{o}C at a heating rate of 2 ^{o}C min^{-1}, dwelled at 240 ^{o}C for 2 h, then heated to 1000 ^{o}C at 5 ^{o}C min^{-1} and dwelled at 1000 ^{o}C for 2 h to allow complete pyrolysis, and then cooled down to room temperature naturally to yield compressible CNFF.

3. Preparation of freestanding graphene film (FGF)

FGF was prepared by exfoliating the nature graphite foil based on our previous work. Typically, graphite foil exfoliation was performed in a homemade two electrode system, whereby graphite foils were used as working anodes and Cu foils as counter electrodes. The electrolyte for the graphite exfoliation was prepared by dispersing ammonium sulfate (0.1 M) in DI water. The electrochemical exfoliation of graphite foil was carried out by applying constant positive voltage (+10 V) on the working electrode. The graphene powder was first collected with cellulose filters and washed repeatedly with DI water and ethanol by vacuum filtration. The washing process was repeated several times to clear any chemical residues. Then, the resultant graphene powder was dispersed in IPA by sonication for 5 h in an ice bath. The dispersion was

kept for 24 h for the precipitation of un-exfoliated graphite flakes. The top part of the dispersion was determined the concentration using the vacuum filtration method. After that, the graphene dispersion was filtered through polyamide membrane filters to obtain a thin film by vacuum-assisted filtration. Then, the film was dried at room temperature and peeled off from the polyamide membrane, which was denoted as FGF.

4. Electrochemical Measurements

The electrochemical performances were conducted using the CR2032 coin type half-cells. The as-prepared CNFF were punched into circular electrodes with a diameter of 6.5 mm and directly used as the working electrodes, and K foil was used as both the counter and reference electrodes. The electrolyte used was a 1.0 M KPF_6 in a mixed solution of ethylene carbonate (EC), dimethyl carbonate (DMC) and ethylmethyl carbonate (EMC) with a volume ratio of 4:3:2. The glass fiber (GF/D) from Whatman was used as the separator. The cells were assembled in an Ar-filled glove box with moisture and oxygen content of less than 0.1 ppm. After cycling tests, batteries were disassembled in the glove box and electrodes were washed with dimethyl carbonate (DMC) completely before being tested. Galvanostatic charge and discharge tests were carried out using a LAND-CT2011A battery-testing instrument at room temperature under different current densities in a voltage range of 0.01-2.8 V vs. K^+/K. Cyclic voltammetry measurements were conducted at a scan rate of 0.1 mV s^{-1} and electrochemical impedance measurements (EIS) were performed in the frequency range from 100 kHz to 0.01 Hz on Biological SP150 Electrochemical Workstation at room temperature.

5. Sample characterization instruments

The morphology of the CNFF was characterized by the scanning electron microscopy (SEM) (Hitachi S4800) and transmission electron microscopy (TEM) (JEOL 1010). High-resolution transmission electron microscopy (HRTEM) and energy dispersive X-ray spectroscopy (EDX) measurements were performed on a JEOL 2010F (Tokyo, Japan) HRTEM at an acceleration voltage of 200 kV. The samples for TEM images were prepared by dropping the dilute colloidal suspension (~0.05 mg mL^{-1}) onto a copper grid and dried in ambient air at room temperature. The SEM images were obtained using a field-emission gun SEM (Quanta 400 FEG FEI) at an

accelerating voltage of 3.0 kV. X-ray diffraction (PANalytical/Philips X'Pert Pro) patterns of CNNF were recorded for 2θ -values ranging from 10^o to 60^o with Cu Kα radiation. Raman spectroscopy was carried out on a LabRam HR800 UV NIR with a 532 nm laser excitation. The nitrogen adsorption-desorption measurements were performed on a Quantachrome ASiQwin-Autosorb Iq Station 2 and the bath temperature was 77.35K (The outgas Temp. is 453.15K). The compression tests were performed on an Instron 5565A testing machine equipped with 500-N and 10000-N compression stages. The strain rate was set at 20 mm min^{-1} for the tests. The specific surface area was calculated at 77 K using BET method.[2]

II. Supplementary Results and Discussion

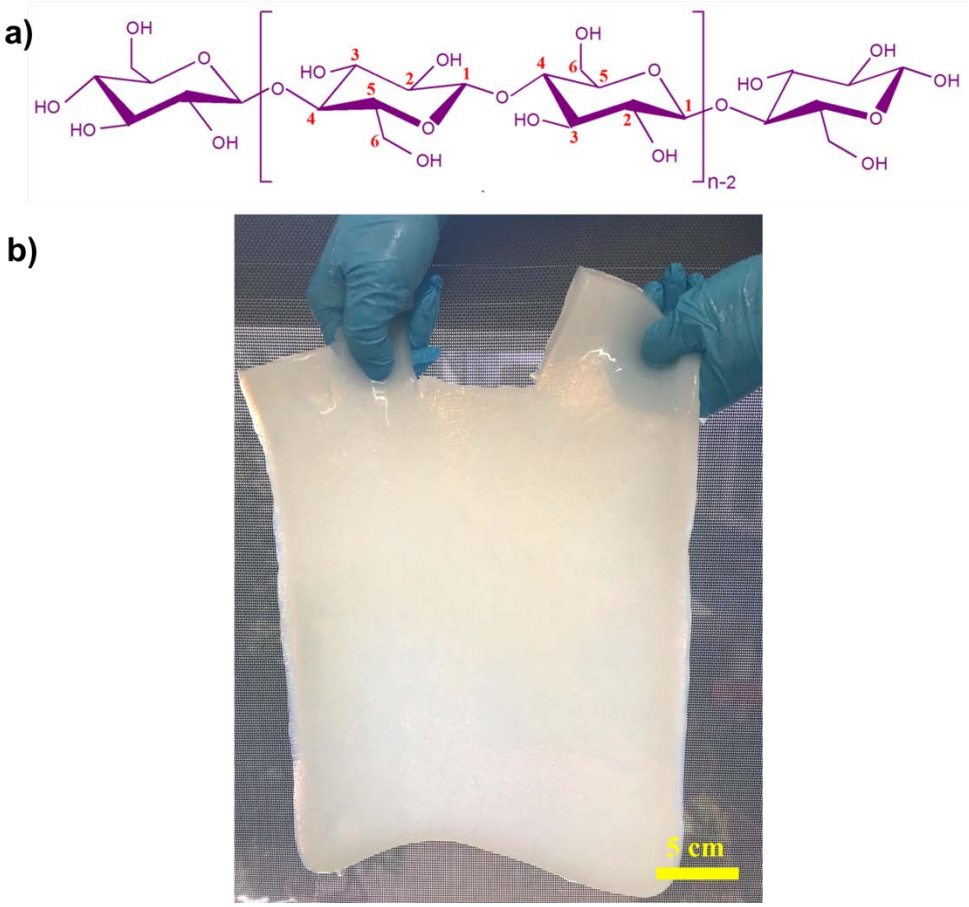

Figure S1 a) The chemical structure of bacterial cellulose. b) BC pellicle are prepared by cutting a piece of purified BC hydrogel into a rectangular shape.

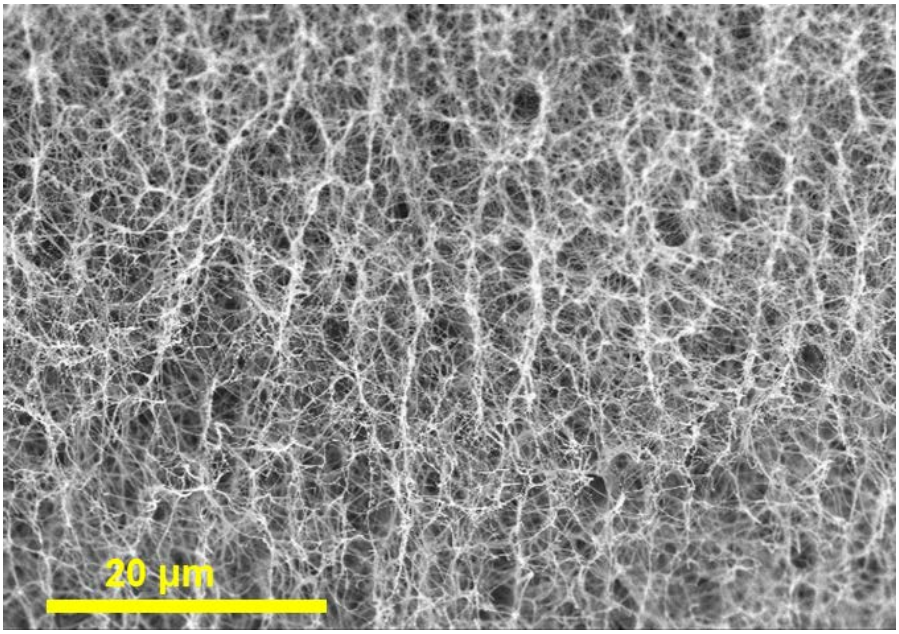

Figure S2 SEM image of original BC aerogel.

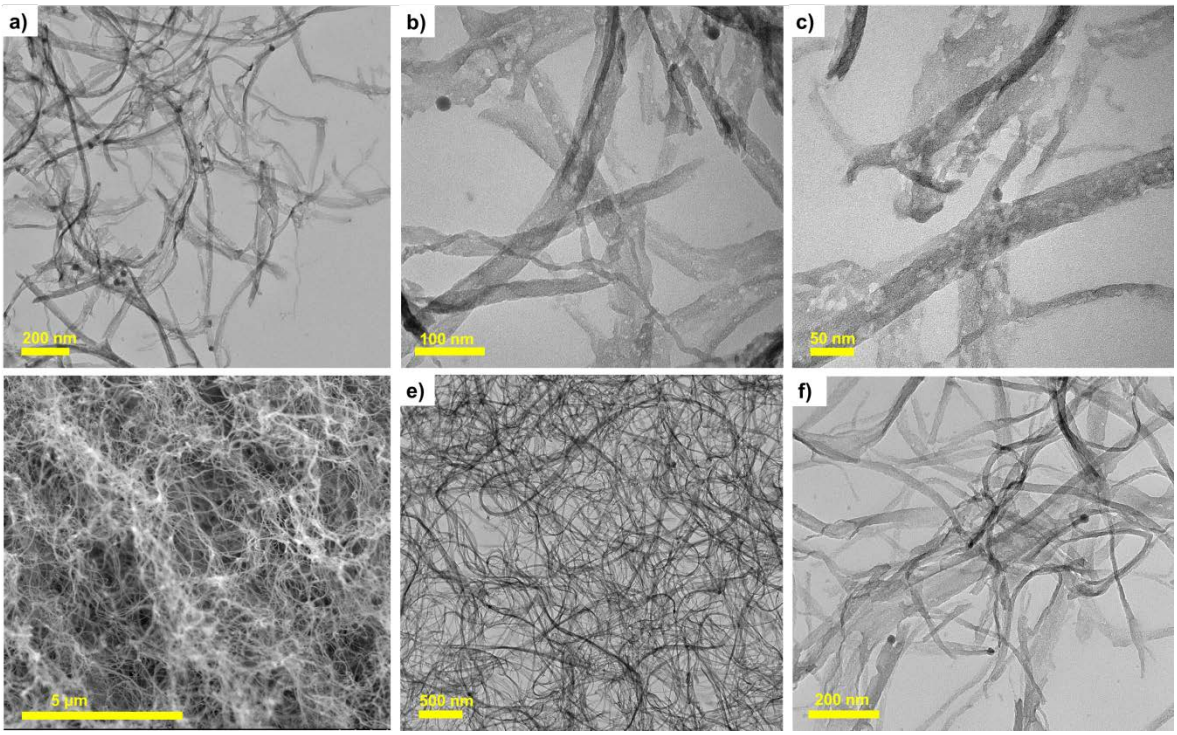

Figure S3 a-c) TEM images showing the first level micropores on the carbon nanofiber. d-e) SEM and TEM images showing the second level micro- and mesopores between the fibers.

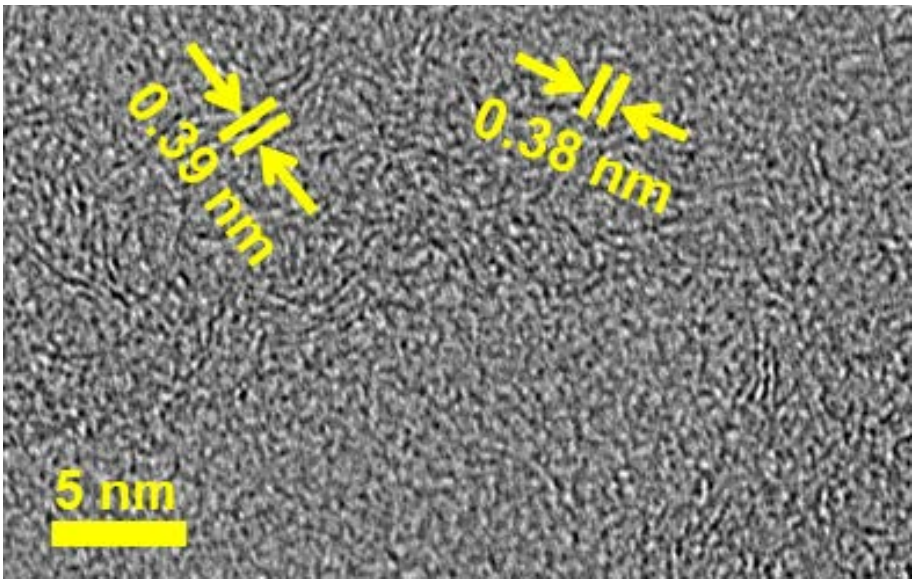

Figure S4 HR-TEM image of CNFF.

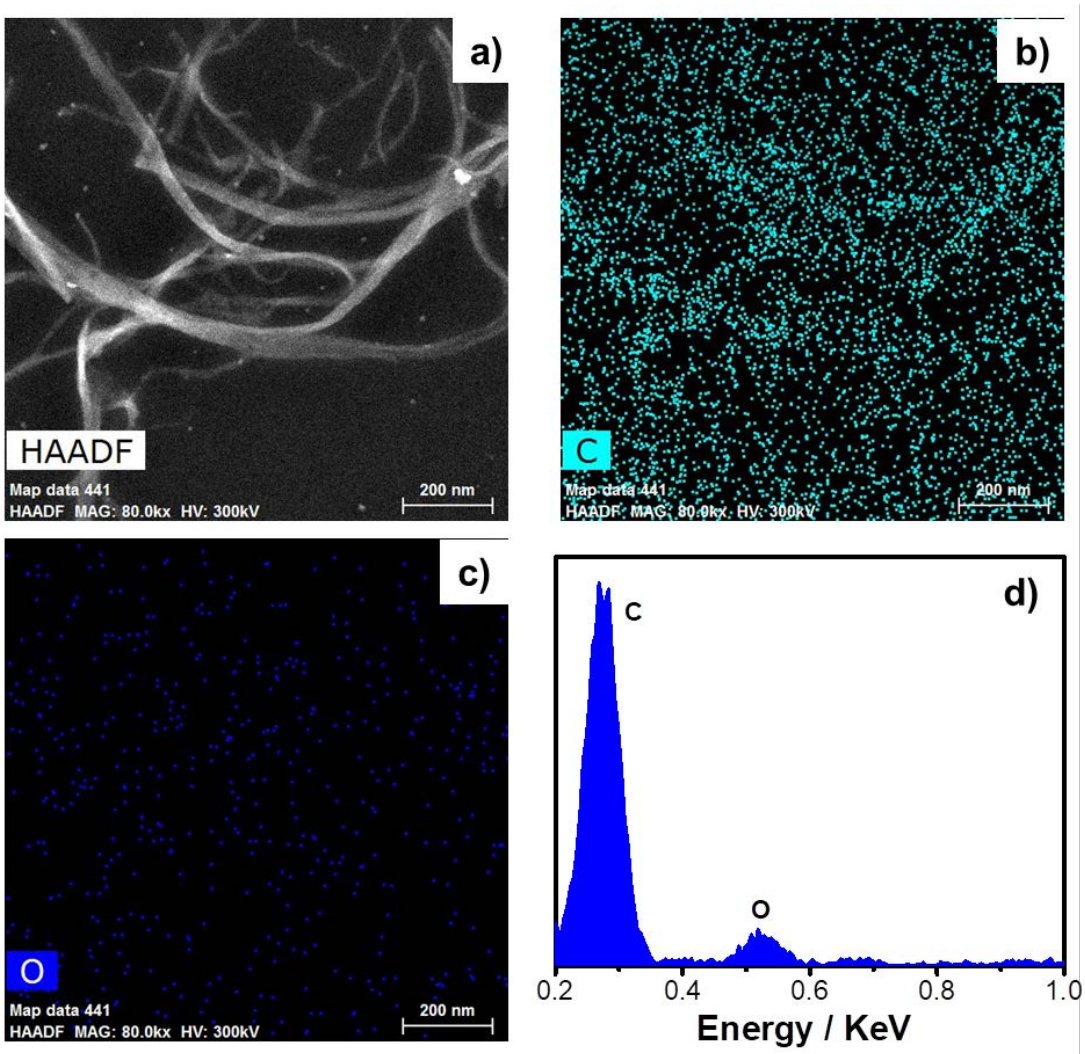

142

143 **Figure S5** a-c) HAADF-STEM and elemental mapping images of b) C, c) O of CNFF. D) The

144 corresponding energy-dispersive X-ray spectrum (EDX) of CNFF.

145

146

147

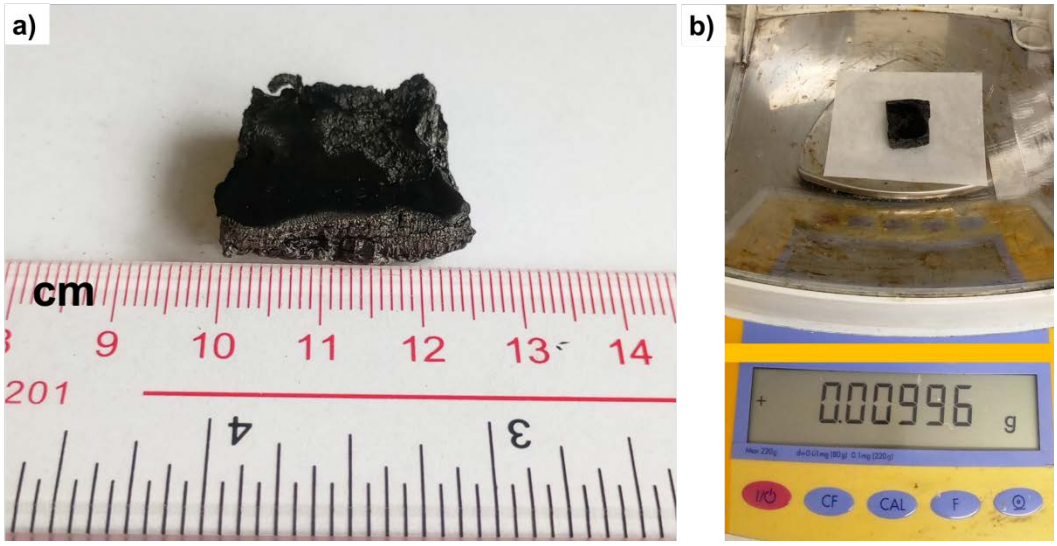

Figure S6 a) Photograph of the dimension of CNFF. b) Photograph of the CNFF on the balance.

Figure S7 Photograph of CNFF in an ethanol flame.

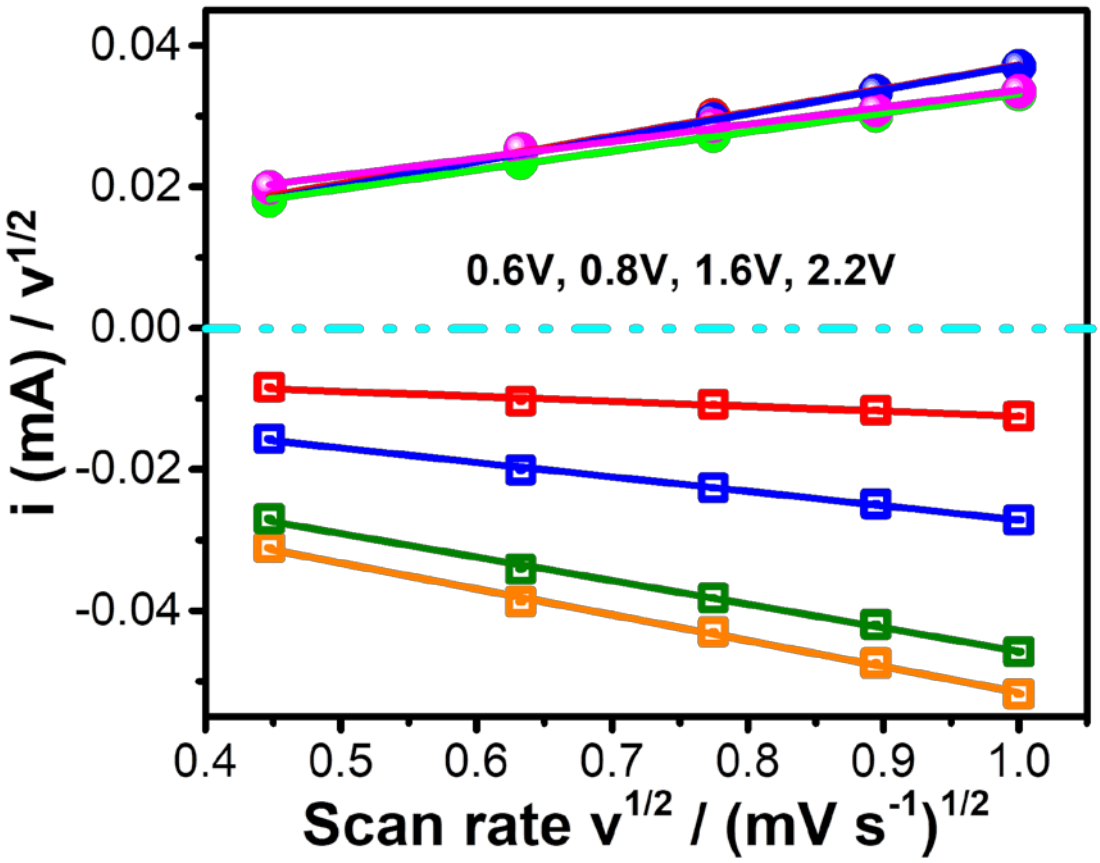

174

175 **Figure S8.** Relationship between i(V)/$v^{1/2}$ *versus* $v^{1/2}$ used for calculating constants k_1 and k_2

176 at different potentials.

177

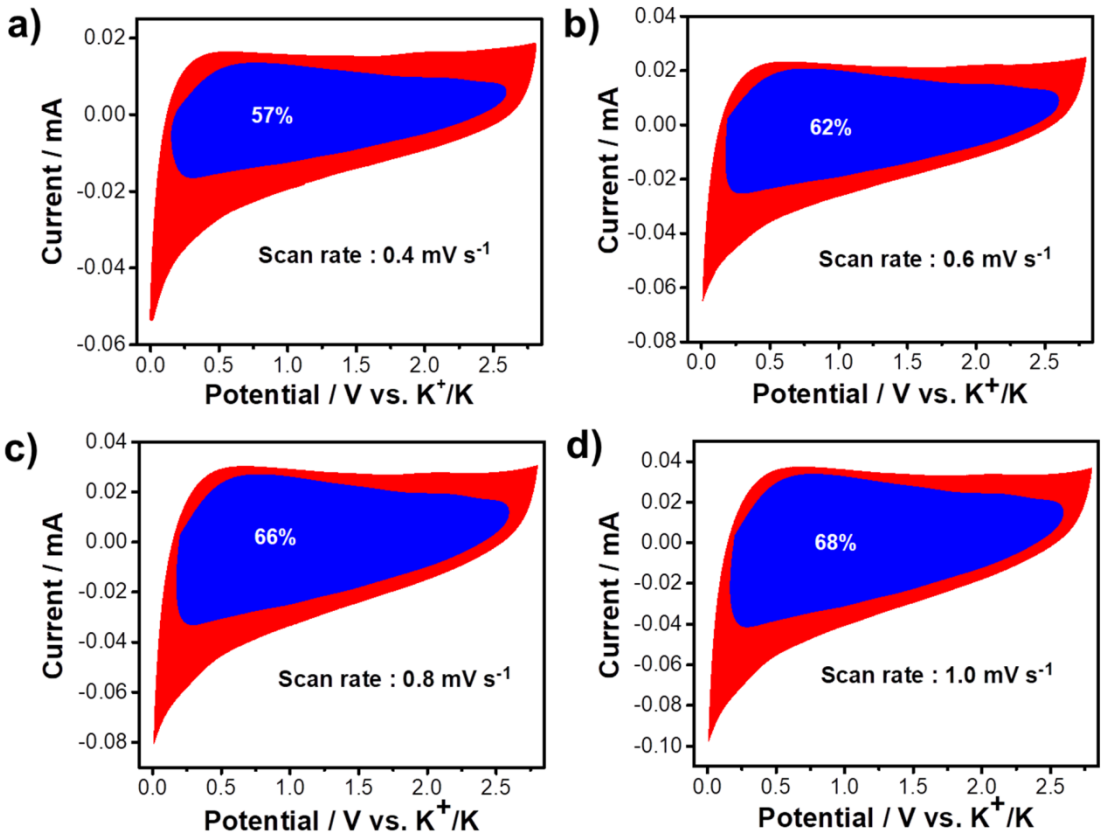

178

179 **Figure S9.** Capacitive charge storage contributions at different scan rates.

180

181

182

183

184

185

186

187

188

189

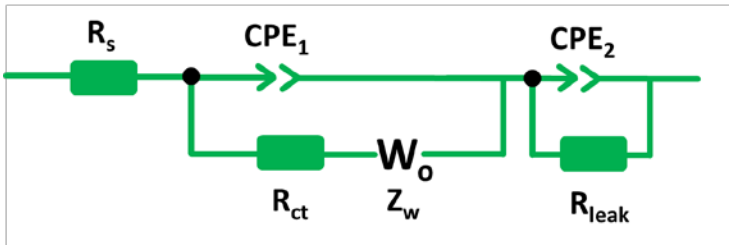

Figure S10. Equivalent circuit model employed to produce the simulation results in the Nyquist plots in different frequency regions. R_s: the equivalent series resistance. R_{ct}: the charge transfer resistance. CPE: a constant phase element. CPE_1 and CPE_2 are capacitor elements from double layer and active material, respectively. Z_w: the Warburg diffusion element. R_{leak}: the leakage resistance associated with the electrode reaction in the bulk.

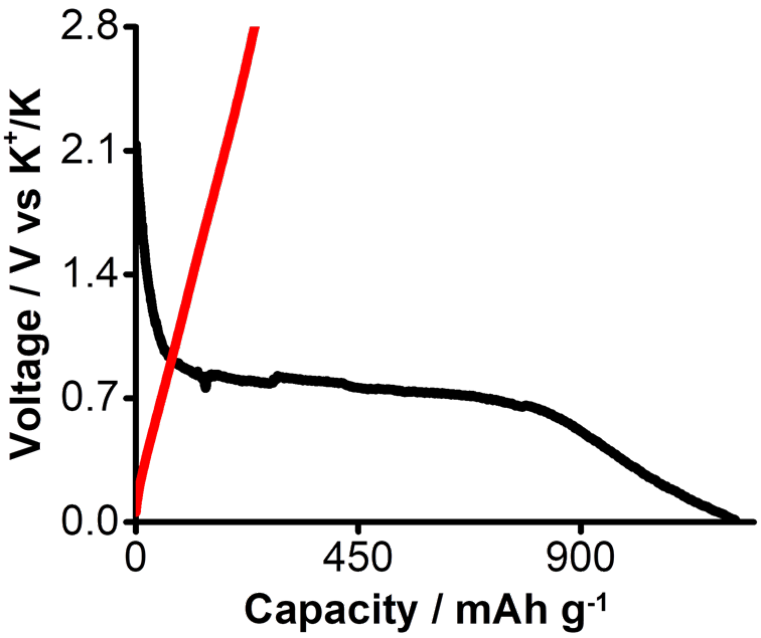

204

205 **Figure S11** The first cycle of the depotasiation and potasiation profiles in PIBs.

206

207

208

209

210

211

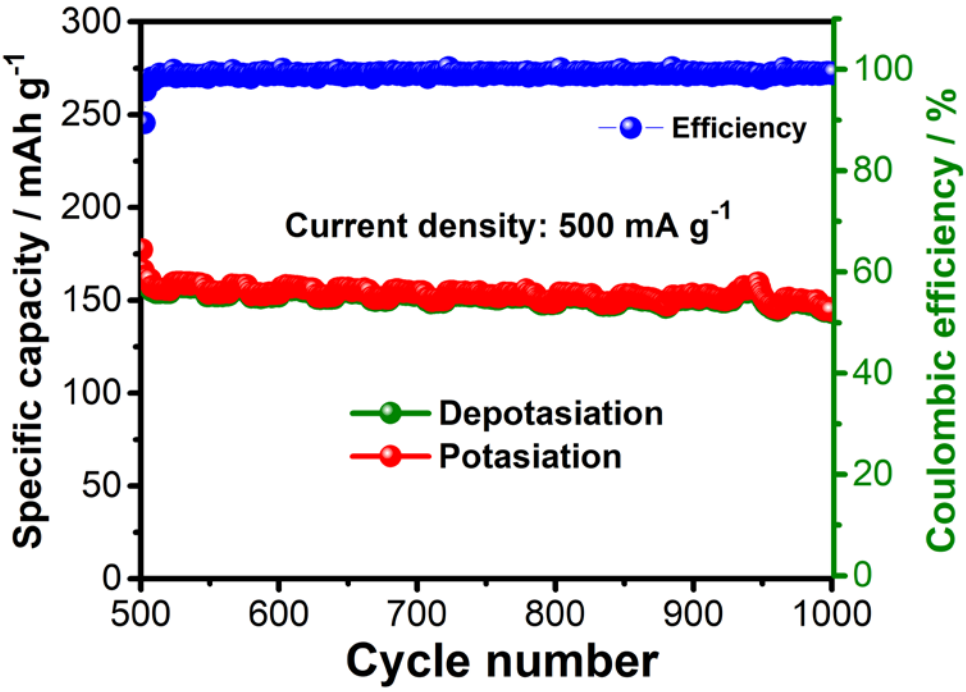

Figure S12. Another long cycling test of CNFF electrode at high current densities of 500 mA g^{-1} after standing 10 days when finish the first 500 cycles at current densities of 500 mA g^{-1}.

Figure S13. Optical image of a LED powered using the CNFF based PIB.

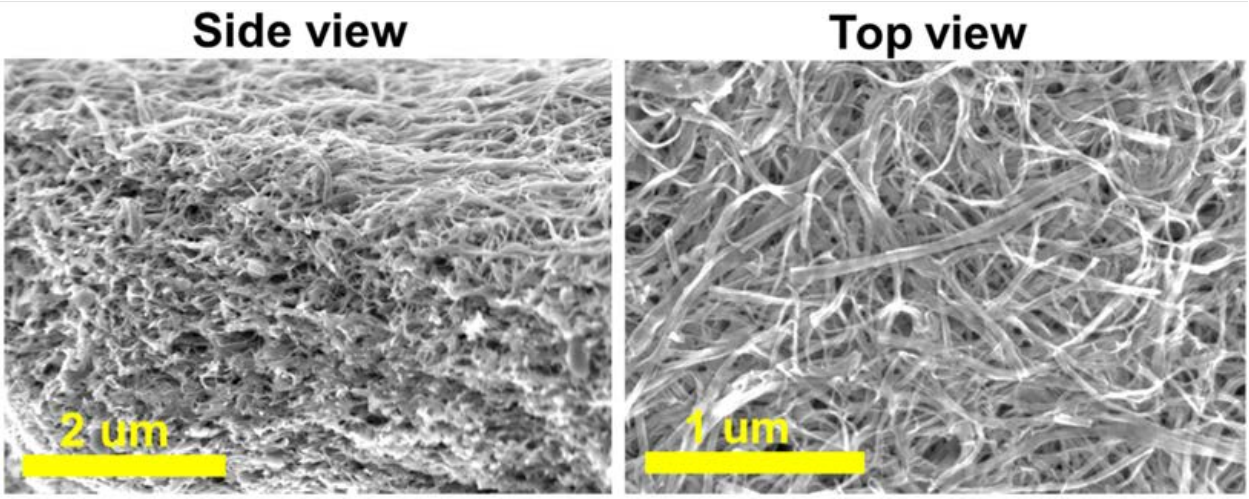

Figure S14. The SEM images of CNFF electrode (side view and top view) after cycled 1000 times at a current density of 500 mA g^{-1}.

Table S1 Cost analysis of the CNFF electrode with commercial carbon foam and graphene foam.

Materials	Price	Size/Weight	Company
BC-derived carbon foam	**$ 8.00**	**Size: 40 cm×25 cm×2 cm;**	**This work**
Graphene	$ 125.00	≥0.2 mg mL^{-1} in DMF; Volume: 50 ml	Sigma-Aldrich
Carbon felt	$ 179.00	Weight: 500-800 g m^{-2}; Size: 2 inch×2 inch; Thickness: 10 mm;	Fuel cell store
3D graphene foam	$ 75.00	Density: 0.2 g cm^{-3}; Thickness: 0.5 mm; Number of layers: 8 layers	ACS material
3D multilayer freestanding graphene foam	$ 250.00	Weight: 0.20 lbs; Size: 2 inch×2 inch; Thickness: 1.2 mm; Pore Size: 580 μm;	Graphene supermarket

Table S2. EIS characteristics of CNFF based PIBs at different cycles (Initial ~1000th) at 500 mA g^{-1}.

Cycle	R_s (Ω)	R_{ct} (Ω)	f_0 (Hz)	τ_0 (s)
Initial	3.3	2037	5.8	0.17
50th	5.8	1531	8.44	0.11
500th	13.68	55.2	9.45	0.10
1000th	7.7	46.17	25	0.04

Table S3. Comparison of cycling performance, rate performance of the CNF foam based PIBs with state-of-the-art material based PIBs performance.

Electrode material	Cycling Performance			Rate Performance		Reference
	Current density (A g^{-1})	Cycles	Capacity (mAh g^{-1})	Current density (A g^{-1})	Capacity (mAh g^{-1})	
				0.05	**240**	
	1.0	**2000**	**158**	**0.1**	**214**	
CNF Foam	**2.0**	**1500**	**141**	**0.2**	**202**	**This work**
	5.0	**1000**	**122**	**0.5**	**181**	
				1.0	**164**	
M-KTO	0.3	900	47	0.3	81	*ACS Nano 2017, 11, 4792-4800.*[3]
$K_2Ti_4O_9$	0.03	10	80	0.1	80	*J. Electrochem. Soc. 2016, 163, A2551-A2554.*[4]
MXene nanoribbons	0.2	500	42	0.3	60	*Nano Energy 2017, 40, 1-8.*[5]
Graphite	0.14	50	100	0.28	80	*J. Am. Chem. Soc. 2015, 137, 11566-11569.*[6]
Graphene	0.1	100	150	0.2	10	*Nanoscale 2016, 8, 16435-16439.*[7]
rGO	0.01	175	150	0.1	50	*Nano lett. 2015, 15, 7671-7677.*[8]
Polynanocrystalline graphite	0.1	240	90	0.5	43	*ACS Appl. Mater . Interfaces 2017, 9, 4343-4351.*[9]
N-FLG	0.1	100	160	0.028	220	*ACS Appl. Mater. Interfaces 2017, 9, 17872-17881.*[10]
N,O doped Hard carbon	1.05	1100	130	3	118	*Adv. Mater. 2018, 30, 1700104.*[11]
Sn-C composite	0.025	30	100	0.025	137	*Chem. Commun. 2016, 52, 9279-9282.*[12]
Few layer N-doped graphene	0.1	100	210	0.2	50	*ACS Nano 2016, 10, 9738-9744.*[13]
Graphite	0.02	200	0	0.5	0	*Adv. Funct. Mater. 2016, 26, 8103-8110.*[14]
Hard-Soft Composite Carbon	0.279	200	118	0.028	261	*Adv. Funct. Mater. 2017, 27, 1700324.*[15]
MoS_2	0.02	10	65.4	0.02	65	*Nano Res. 2017, 10, 1313-1321.*[16]
Expanded graphite	0.05	200	228	0.2	175	*J. Power Sources 2018, 378, 66-72.*[17]

Hard-wood-based hard carbon	0.1	160	140	0.1	135	*J. Electrochem. Soc. 2017, 164, A2012-A2016.*[18]
Activated carbon	0.2	100	100	1.0	30	*Carbon 2017, 123, 54-61.*[19]
N-doped carbon nanofibers	0.055	100	200	0.558	109.3	*Carbon 2018, 128, 224-230.*[20]
$K_2Ti_8O_{17}$	0.02	50	110.7	0.02	182	*Chem. Commun., 2016, 52, 11274-11276.*(21)

III. References.

(1) M. Wang, Y. Yang, Z. Yang, L. Gu, Q. Chen, Y. Yu, *Adv. Sci.* **2017**, *4*, 1600468.

(2) L. Yang, A. Mukhopadhyay, Y. Jiao, Q. Yong, L. Chen, Y. Xing, J. Hamel, H. Zhu, *Nanoscale* **2017**, *9*, 11452-11462.

(3) Y. Dong, Z.-S. Wu, S. Zheng, X. Wang, J. Qin, S. Wang, X. Shi, X. Bao, *ACS Nano* **2017**, *11*, 4792-4800.

(4) B. Kishore, G. Venkatesh, N. Munichandraiah, *J. Electrochem. Soc.* **2016**, *163*, A2551-A2554.

(5) P. Lian, Y. Dong, Z.-S. Wu, S. Zheng, X. Wang, S. Wang, C. Sun, J. Qin, X. Shi, X. Bao, *Nano Energy* **2017**, *40*, 1-8.

(6) Z. Jian, W. Luo, X. Ji, *J. Am. Chem. Soc.* **2015**, *137*, 11566-11569.

(7) K. Share, A. P. Cohn, R. E. Carter, C. L. Pint, *Nanoscale* **2016**, *8*, 16435-16439.

(8) W. Luo, J. Wan, B. Ozdemir, W. Bao, Y. Chen, J. Dai, H. Lin, Y. Xu, F. Gu, V. Barone, *Nano Lett.* **2015**, *15*, 7671-7677.

(9) Z. Xing, Y. Qi, Z. Jian, X. Ji, *ACS Appl. Mater. Interfaces* **2016**, *9*, 4343-4351.

(10) R. A. Adams, J.-M. Syu, Y. Zhao, C. T. Lo, A. Varma, V. G. Pol, *ACS Appl. Mater. Interfaces* **2017**, *9*, 17872-17881.

(11) J. Yang, Z. Ju, Y. Jiang, Z. Xing, B. Xi, J. Feng, S. Xiong, *Adv. Mater.*. **2018**, *30*, 1700104.

(12) I. Sultana, T. Ramireddy, M. M. Rahman, Y. Chen, A. M. Glushenkov, *Chem.Commun.* **2016**, *52*, 9279-9282.

(13) K. Share, A. P. Cohn, R. Carter, B. Rogers, C. L. Pint, *ACS Nano* **2016**, *10*, 9738-9744.

(14) J. Zhao, X. Zou, Y. Zhu, Y. Xu, C. Wang, *Adv. Funct. Mater.* **2016**, *26*, 8103-8110.

(15) Z. Jian, S. Hwang, Z. Li, A. S. Hernandez, X. Wang, Z. Xing, D. Su, X. Ji, *Adv. Funct. Mater.* **2017**, *27*, 1700324.

(16) X. Ren, Q. Zhao, W. D. McCulloch, Y. Wu, *Nano Res.* **2017**, *10*, 1313-1321.

(17) Y. An, H. Fei, G. Zeng, L. Ci, B. Xi, S. Xiong, J. Feng, *J. Power Sources* **2018**, *378*, 66-72.

(18) S. R. Prabakar, S. C. Han, C. Park, I. A. Bhairuba, M. J. Reece, K.-S. Sohn, M. Pyo, *J. The Electrochem.Soc.* **2017**, *164*, A2012-A2016.

(19) Z. Tai, Q. Zhang, Y. Liu, H. Liu, S. Dou, *Carbon* **2017**, *123*, 54-61.

(20) R. Hao, H. Lan, C. Kuang, H. Wang, L. Guo, *Carbon* **2018**, *128*, 224-230.

(21) J. Han M. Xu, Y. Niu G.Li, M. Wang, Y. Zhang, M. Jia, C. Li, *Chem. Commun.*, **2016**, 52, 11274-11276.